PHYSICAL REVIEW D **86,** 096006 (2012)

Study of beta equilibrated 2 + 1 flavor quark matter in the Polyakov-Nambu-Jona-Lasinio model

Abhijit Bhattacharyya*
Department of Physics, University of Calcutta, 92, A.P.C Road, Kolkata 700009, India

Sanjay K. Ghosh,† Sarbani Majumder,‡ and Rajarshi Ray§
Center for Astroparticle Physics and Space Science, Block-EN, Sector-V, Salt Lake, Kolkata 700091, India and Department of Physics, Bose Institute, 93/1, A.P.C Road, Kolkata 700009, India
(Received 29 July 2011; published 19 November 2012)

We report the first case study of the phase diagram of 2 + 1 flavor strongly interacting matter in β equilibrium, using the Polyakov-Nambu-Jona-Lasinio model. Physical characteristics of relevant thermodynamic observables have been discussed. A comparative analysis with the corresponding observables in the Nambu-Jona-Lasinio model is presented. We find distinct differences between the models in terms of a number of thermodynamic quantities like the speed of sound, specific heat, various number densities, as well as entropy. The present study is expected to give us a better insight into the role that the superdense matter created in heavy-ion collision experiments plays in our understanding of the properties of matter inside the core of supermassive stars in the Universe.

DOI: 10.1103/PhysRevD.86.096006 PACS numbers: 25.75.Nq, 21.65.Qr, 26.60.Kp

I. INTRODUCTION

The phase diagram of strongly interacting matter has been at the center of attention for quite some time now. Under a variety of extreme conditions of temperature and/or density the hadrons may overlap and lose their individuality and a new state of matter called quark gluon plasma may be formed [1]. It is well believed that such a state of matter existed in the hot early Universe, a few microseconds after the big bang. Deconfined quark matter could also exist in the core of neutron stars (NSs) [2–4] where the temperature is relatively low but density is high. So an understanding of the physics of strongly interacting matter at such environmental conditions would have important cosmological and astrophysical significance.

In the laboratory such conditions of large temperatures and densities can be created by the collision of heavy ions at high energies. Presently the strongly interacting matter at high temperature and close to zero baryon densities—a scenario relevant for the early universe—is being explored at Relativistic Heavy Ion Collider (RHIC) at Brookhaven National Laboratory and the Large Hadron Collider at CERN. A wealth of information has been obtained from the RHIC, and a lot more is expected from both the future runs there as well as from the Large Hadron Collider. More recently a variety of energy scans at the RHIC and the upcoming facility (facility for antiproton and ion research) at Gesellschaft für Schwerionenforschung are expected to give us a glimpse of matter in the baryon-rich environments—the so-called *compressed baryonic matter*. These experiments will also be useful in the search for signatures of critical phenomena associated with a second order critical end point (CEP).

At the same time, observational data are being collected by a large number of telescopes and satellites [5] such as the radio telescopes at the Arecibo, Parkes, Jodrell Bank, and Green Bank Observatories, the Hubble Space Telescope, European Space Agency's International Gamma Ray Astrophysics Laboratory satellite, Very Large Telescope of the European Southern Observatory, the x-ray satellites Chandra, XMM-Newton, and NASA's Rossi X-ray Timing Explorer, and the Swift satellite. Observations from these facilities are supposed to tell us about the properties of strongly interacting matter at high densities relevant for the astrophysics of compact stars.

Thus on one hand the laboratory experiments are expected to scan the phase space temperature and various conserved quantum number densities of strongly interacting matter. On the other hand the astrophysical observations are expected to uncover the physics for the high baryon number density region of the phase diagram. It should be noted here that the physical characteristics of the matter under consideration may be quite different in the two cases. The time scale of the dynamics of heavy-ion experiments is so small that only strong interactions may equilibrate thermodynamically, while the dynamics in the astrophysical scenario is slow enough to allow even weak interactions to equilibrate. Thus a question naturally arises—to what extent can laboratory experiments be used to infer about the compact star interiors? The aim of this paper is to address this question at a preliminary level from the characteristics of the "β equilibrated" phase diagrams.

One should be able to study the properties of systems described above from first principles using quantum

*abphy@caluniv.ac.in
†sanjay@bosemain.boseinst.ac.in
‡sarbanimajumder@gmail.com
§rajarshi@bosemain.boseinst.ac.in

chromodynamics (QCD), which is *the* theory of strong interactions. However, QCD is highly nonperturbative in the region of temperature and density that we are interested in. The most reliable way to analyze the physics in this region of interest is to perform a numerical computation of the lattice version of QCD (lattice QCD). The scheme is robust but numerically costly. Moreover, there are problems in applying this scheme for the systems having finite baryon density. Thus it has become a common practice to study the physics of strongly interacting matter under the given conditions using various QCD inspired effective models.

Until now various quark models, such as different versions of the Massachusetts Institute of Technology bag model [6,7], the color-dielectric model [8,9], and different formulations of the Nambu-Jona-Lasinio (NJL) model [10,11] have been used to study the NS structure. Despite the similarity of the results on the value of the maximum NS mass, the predictions on the NS configurations can differ substantially from model to model. The most striking difference is in the quark matter content of the NSs, which can be extremely large in the case of the equation of state (EOS) related to the massachusetts institute of technology bag model or the color-dielectric model, but it is vanishingly small in the case of the original version of the NJL model [10,12]. In the case of the NJL model it turns out that, as soon as quark matter appears at increasing NS mass, the star becomes unstable, with only the possibility of a small central region with a mixed phase of nucleonic and quark matter. This may be a result of the lack of confinement in the NJL model. In fact an indirect relationship between confinement and NS stability has been found in a study using the NJL model with density dependent cutoff [13]. Hence it is important to study the EOS from the Polyakov-Nambu-Jona-Lasinio (PNJL) model [14–16], where a better description of confinement has been incorporated through the Polyakov loop mechanism. Moreover, a comparison with the NJL model might be helpful in understanding the role of the Polyakov loop at high chemical potential.

A detailed study of $2 + 1$ flavor strong interactions has been done by some of us using the PNJL model. The general thermodynamic properties along with the phase diagram [17], as well as details of fluctuation and correlations of various conserved charges [18], have been reported. Here we extend the work by including β equilibrium into the picture. In the context of the NJL model such a study was done earlier in Refs. [19,20]. The properties of pseudoscalar and neutral mesons have been studied in the finite density region within the framework of a $2 + 1$ flavor NJL model in β-equilibrium [21,22].

We investigate and compare different properties of the NJL and PNJL models in the T-μ_B plane. The specialization of these studies to the possible dynamical evolution of NSs and/or compressed baryonic matter created in heavy-ion collisions will be kept as a future exercise.

The paper is organized as follows. In Sec. II we discuss our model. In Sec. III we calculate different thermodynamic properties and present our result and finally we conclude in Sec. IV.

II. FORMALISM

The supermassive compact objects like neutron stars are born in the aftermath of supernova explosions. The initial temperature of a newborn NS can be as high as $T \sim 100$ MeV. For about one minute following its birth, the star stays in a special protoneutron star state: hot, opaque to neutrinos, and larger than an ordinary NS (see, e.g., Refs. [23,24] and references therein). Later the star becomes transparent to neutrinos generated in its interior. It cools down gradually, initially through neutrino emission ($t \leq 10^5$ years) and then through the emission of photons ($t \geq 10^5$ years) [25], and transforms into an ordinary NS. The weak interaction responsible for the emission of these neutrinos eventually drives the stars to the state of β equilibrium along with the imposed condition of charge neutrality.

The mass, radius, and other characteristics of such a star depend on the EOS, which in turn is determined by the composition of the star [26]. The possible central density of a compact star may be high enough for the usual neutron-proton matter to undergo a phase transition to some exotic forms of strongly interacting matter. Some of the suggested exotic forms of strongly interacting matter are the hyperonic matter, the quark matter, the superconducting quark matter, etc. If there is a hadron to quark phase transition inside the NS, then all the characteristics of the NS will depend on the nature of the phase transition [27,28].

Furthermore, there have been suggestions that the strange quark matter, containing almost equal numbers of u, d, and s quarks, may be the ground state of strongly interacting matter (see Ref. [29] and references therein). If such a conjecture is true, then there is a possibility of the existence of self-bound pure strange stars as well. In fact, the conversion of NSs to a strange star may really be a two step process [30]. The first process involves the deconfinement of nuclear to two flavor quark matter; the second process deals with the conversion of excess down quarks to strange quarks resulting into a β equilibrated charge neutral strange quark matter. There are several mechanisms by which the conversion of a strange quark may be triggered at the center of the star [31,32]. The dominant reaction mechanism by which the strange quark production in quark matter occurs is the nonleptonic weak interaction process [33]:

$$u_1 + d \leftrightarrow u_2 + s. \tag{1}$$

Initially when the quark matter is formed, $\mu_d > \mu_s$, and the above reaction converts excess d quarks to s quarks. But in order to produce chemical equilibrium the semileptonic interactions,

$$d(s) \rightarrow u + e^- + \bar{\nu}_e, \tag{2}$$

$$u + e^- \rightarrow d(s) + \nu_e, \tag{3}$$

play an important role along with the above nonleptonic interactions. These imply the β-equilibrium condition $\mu_d = \mu_u + \mu_e + \mu_{\bar{\nu}}$ and $\mu_s = \mu_d$.

Actually, the only conserved charges in the system are the baryon number n_B and the electric charge n_Q. Since we are assuming neutrinos to leave the system, lepton number is not conserved [10]. Strange chemical potential μ_S is zero because strangeness is not conserved. So two of the four chemical potentials (μ_u, μ_d, μ_s, and μ_e) are independent. In terms of the baryon chemical potential (μ_B), which is equivalent to the quark chemical potential ($\mu_q = \mu_B/3$), and the charge chemical potential (μ_Q), these can be expressed as $\mu_u = \mu_q + \frac{2}{3}\mu_Q$, $\mu_d = \mu_q - \frac{1}{3}\mu_Q$, $\mu_s = \mu_q - \frac{1}{3}\mu_Q$, $\mu_e = -\mu_Q$. These conditions are put as constraints in the description of the thermodynamics of a given system through the PNJL model.

The thermodynamic potential of the 2 + 1 flavor PNJL model for nonzero quark chemical potential is [17]

$$\begin{aligned}\Omega = {} & \mathcal{U}'[\Phi, \bar{\Phi}, T] + 2g_S \sum_{f=u,d,s} \sigma_f^2 - \frac{g_D}{2}\sigma_u\sigma_d\sigma_s - 6\sum_{f=u,d,s}\int_0^\Lambda \frac{d^3p}{(2\pi)^3} E_f \Theta(\Lambda - |\vec{p}|) \\ & - 2T\sum_{f=u,d,s}\int_0^\infty \frac{d^3p}{(2\pi)^3}\ln\Big[1 + 3\Big(\Phi + \bar{\Phi}e^{-\frac{(E_f-\mu_f)}{T}}\Big)e^{-\frac{(E_f-\mu_f)}{T}} + e^{-3\frac{(E_f-\mu_f)}{T}}\Big] \\ & - 2T\sum_{f=u,d,s}\int_0^\infty \frac{d^3p}{(2\pi)^3}\ln\Big[1 + 3\Big(\bar{\Phi} + \Phi e^{-\frac{(E_f+\mu_f)}{T}}\Big)e^{-\frac{(E_f+\mu_f)}{T}} + e^{-3\frac{(E_f+\mu_f)}{T}}\Big],\end{aligned} \tag{4}$$

where $\sigma_f = \langle\bar{\psi}_f\psi_f\rangle$ and $E_f = \sqrt{p^2 + M_f^2}$ with $M_f = m_f - 2g_S\sigma_f + \frac{g_D}{2}\sigma_{f+1}\sigma_{f+2}$.

The effective potential $\mathcal{U}'(\Phi, \bar{\Phi}, T)$ is expressed in terms of the traced Polyakov loop $\Phi = (\mathrm{Tr}_c L)/N_c$ and its (charge) conjugate $\bar{\Phi} = (\mathrm{Tr}_c L^\dagger)/N_c$, where L is a matrix in color space given by $L(\vec{x}) = \mathcal{P}\exp[-i\int_0^\beta d\tau A_4(\vec{x}, \tau)]$, where $\beta = 1/T$ is the inverse temperature and $A_4 = A_4^a\lambda_a$, A_4^a being the temporal component of the Eucledian gluon field and λ_a the Gell-Mann matrices with adjoint color indices $a = 1, \ldots, 8$. Assuming a constant A_4^a and the A_i's to be zero for ($i = 1, 2, 3$), Φ and its conjugate $\bar{\Phi}$ are treated as classical field variables in the PNJL model. The temperature dependent effective potential $\mathcal{U}'(\Phi, \bar{\Phi}, T)$ is so chosen to have exact $Z(3)$ center symmetry and is given by

$$\frac{\mathcal{U}'(\Phi, \bar{\Phi})}{T^4} = \frac{\mathcal{U}(\Phi, \bar{\Phi})}{T^4} - \kappa\ln[J(\Phi, \bar{\Phi})], \tag{5}$$

where

$$\begin{aligned}\frac{\mathcal{U}(\Phi, \bar{\Phi}, T)}{T^4} = {} & -\frac{b_2(T)}{2}\bar{\Phi}\Phi - \frac{b_3}{6}(\Phi^3 + \bar{\Phi}^3) \\ & + \frac{b_4}{4}(\bar{\Phi}\Phi)^2\end{aligned} \tag{6}$$

with $b_2(T) = a_0 + a_1(\frac{T_0}{T}) + a_2(\frac{T_0}{T})^2 + a_3(\frac{T_0}{T})^3$, and $J[\Phi, \bar{\Phi}] = (27/24\pi^2)(1 - 6\bar{\Phi}\Phi + 4(\bar{\Phi}^3 + \Phi^3) - 3(\bar{\Phi}\Phi)^2)$ the Vandermonde determinant. A fit of the coefficients a_i, b_i is performed to reproduce the pure-gauge lattice data and $T_0 = 270$ MeV is adopted in our work. Finally $\kappa = 0.2$ is used which gives reasonable values for pressure for the temperature range used here at zero baryon density as compared to full lattice QCD computations.

For simplicity, electrons are considered as free noninteracting fermions [10] and the corresponding thermodynamic potential is

$$\Omega_e = -\Big(\frac{{\mu_e}^4}{12\pi^2} + \frac{{\mu_e}^2T^2}{6} + \frac{7\pi^2T^4}{180}\Big), \tag{7}$$

where μ_e is the electron chemical potential.

III. RESULTS AND DISCUSSIONS

The thermodynamic potential Ω is extremized with respect to the scalar fields under the condition $\mu_d = \mu_u + \mu_e$ and $\mu_s = \mu_d$. The equations of motions for the mean fields σ_u, σ_d, σ_s, Φ, and $\bar{\Phi}$ for any given values of temperature T, quark chemical potential μ_q, and electron chemical potential μ_e are determined through the coupled equations,

$$\begin{aligned}&\frac{\partial\Omega}{\partial\sigma_u} = 0, \quad \frac{\partial\Omega}{\partial\sigma_d} = 0, \quad \frac{\partial\Omega}{\partial\sigma_s} = 0, \\ &\frac{\partial\Omega}{\partial\Phi} = 0, \quad \frac{\partial\Omega}{\partial\bar{\Phi}} = 0.\end{aligned} \tag{8}$$

In Fig. 1, we show the typical variation of constituent quark masses as a function of μ_q, for two representative values of electron chemical potential $\mu_e = 0$ MeV and $\mu_e = 40$ MeV, with a fixed temperature $T = 50$ MeV. At this temperature, both m_u and m_s in the PNJL model show a discontinuous jump at around $\mu_q = 350$ MeV indicating a first order phase transition. The jump in m_s is smaller, and is actually a manifestation of chiral

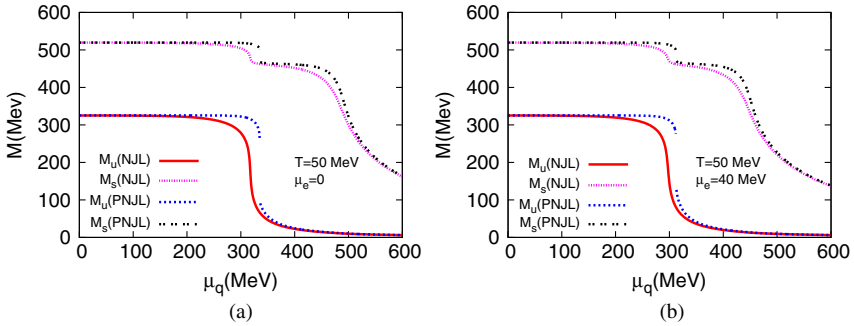

FIG. 1 (color online). Constituent quark masses as functions of μ_q for (a) $\mu_e = 0$ MeV and (b) $\mu_e = 40$ MeV, at $T = 50$ MeV.

transition in the two flavor sector, arising due to the coupling of the strange condensate to the light flavor condensates. On the other hand in the NJL model the quark masses show a smooth variation at this temperature, indicating a crossover. It is important to note that the constituent mass of the strange quark goes down to the current mass at a larger μ_q in both the models, leading to sort of a second crossover at around $\mu_q = 500$ MeV. This will have important implications for some of the thermodynamic observables as we discuss below.

The phase diagrams for NJL and PNJL models are obtained from the behavior of the mean fields, and are shown in Figs. 2(a) and 2(b) for $\mu_e = 0$ MeV and $\mu_e = 40$ MeV, respectively. As is evident from the figures, the broad features of the phase diagrams remain the same in all cases. The difference between the NJL and PNJL models arises mainly due to the Polyakov loop, whose presence is primarily responsible for raising the transition/crossover temperature in the PNJL model. Thus the CEP for the PNJL model occurs at slightly higher T and lower μ_q compared to the NJL model. Note that the phase diagram with $\mu_e = 0$ MeV is identical to the case without β equilibrium [17]. This is because the minimization conditions (8) are independent of the electrons except through the β-equilibrium conditions. However this is true only so far as the phase diagram is concerned. Various other physical quantities are found to differ even for $\mu_e = 0$ as discussed below. For nonzero μ_e we find a slight lowering of the temperature for the CEP by about 10 MeV. This is an important quantitative difference between the physics of neutron stars and that of compressed baryonic matter created in the laboratory. It is worth mentioning that the CEP we have obtained corresponds to the chiral phase transition. Generally in the standard QCD phase diagram, the chiral and deconfinement phase transitions are shown by a single boundary. However it was argued and elucidated that the two transition lines in the T-μ_B plane are distinct [34,35]. In this context we would like to mention that in Ref. [36] the QCD phase diagram has been studied both for isospin asymmetric and symmetric situations, although they have not considered the β-equilibrium scenario. The authors used a two equation of state model, a nonlinear Walecka model, to describe the hadronic sector and (P)NJL model for the quark sector. It has been shown in Ref. [36] that CEP remains unaffected by the isospin asymmetry and the authors found it to be quite generic for a two EOS model.

The system under investigation can be characterized primarily by the behavior of the EOS. Generally for a many body system, an increase in pressure at large densities is indicative of a repulsive behavior of the interaction at large densities (large μ_q) or short distances and an attractive nature at larger distances or lower densities [37,38]. Consequentially the energy density will show

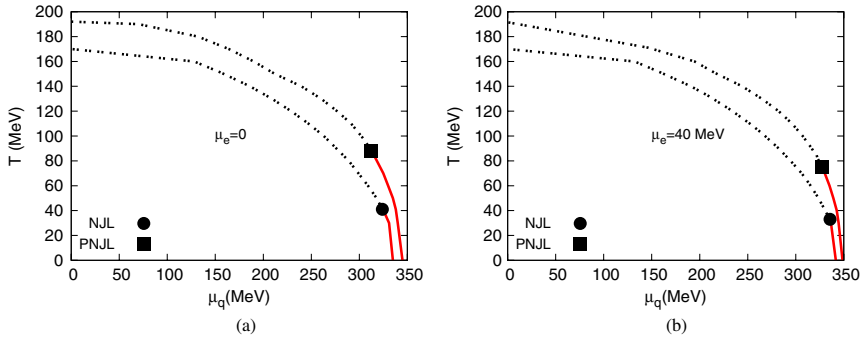

FIG. 2 (color online). Comparison of phase diagram in the NJL and PNJL models at β equilibrium for (a) $\mu_e = 0$ and (b) $\mu_e = 40$. The solid circle and square represent the CEP for the NJL and PNJL models, respectively.

similar behavior. The resulting EOS given by the variation of pressure P with energy density ϵ is shown in Fig. 3(a) at $T = 50$ MeV, for both the NJL and PNJL models, for the two representative electron chemical potentials. Here again for the PNJL model there exists a discontinuity due to a first order nature of the transition, whereas for the NJL model the EOS is smooth. Beyond this region a smaller steepening in ϵ is visible, that occurs due to a second crossover feature noted above as the strange quark condensate starts to melt. A possible implication for this small surge may be that in a strange quark star, at a given central density, the pressure would be somewhat lesser than the situation without this surge.

Generally, the EOS can be used to study the dynamics of a neutron star and that of heavy-ion collisions through the respective flow equations. The main differences would be due to the presence of β equilibrium and the backreaction of the nontrivial space-time metric on the EOS for neutron stars. Such a comprehensive comparative study will be taken up in a later work.

In Fig. 3(b), the variation of the isentropic speed of sound squared $c_s^2 = \partial P/\partial\epsilon$ is plotted against μ_q at $T = 50$ MeV. In the NJL model the c_s^2 starts from a nonzero value, steadily decreases, and then shows a sharp fall around the crossover region at $\mu_q \sim 320$ MeV. This is followed by a sharp rise, a dip, and then approaches the ideal gas value of $1/3$. In contrast the c_s^2 in the PNJL model starting from the ideal gas value remains almost constant up to $\mu_q \sim 200$ MeV and then falls sharply to almost zero. This is followed by a discontinuous jump, a similar dip at $\mu_q \sim 500$ MeV, and a gradual approach to a nonzero value quite different from the ideal gas limit.

The difference at $\mu_q = 0$ MeV occurs specifically due to the Polyakov loop which suppresses any quarklike quasiparticles. As a result the c_s^2 is completely determined by the ideal electron gas. On the other hand those quasiparticles with heavy constituent masses tend to lower the c_s^2 in the NJL model. The difference at the transition region is again mainly due to the discontinuous phase transition in the PNJL model which leads to c_s^2 almost going down to zero, and a crossover in the NJL model where c_s^2 is small but nonzero. In Ref. [39] it was noted that for two conserved charges, pressure is not constant any more in the mixed phase, rather its variation becomes slower, resulting in a smaller but nonzero speed of sound. In our computation, though, we do not find c_s^2 exactly equal to zero, but to confirm such an effect we need a full space-time simulation of the mixed phase through the process of bubble nucleation which is beyond the scope of the present work.

In both the models the dip around $\mu_q = 500$ MeV arises due to the behavior of the strange quark condensate as discussed earlier. If it were possible to achieve such extremely high densities in heavy-ion experiments, then such a dip would slow down the flow and would result in a larger fire ball lifetime. At even higher μ_q the c_s^2 in the NJL model approaches the free field limit quite fast but in the PNJL model it still remains quite low due to the nontrivial interaction brought in by the Polyakov loop. It would be interesting to study the implication of the slow speed of sound inside the core of a neutron star.

Commensurate with the relative stiffening of the equation of state we find that the compressibility $\kappa = \frac{1}{n_q^2}(\frac{\partial n_q}{\partial \mu_q})_T$, where n_q is the quark number density, behaves accordingly. While κ in the NJL model is found to be higher than that of the PNJL model in the hadronic phase, it is just the opposite in the partonic phase as shown in Fig. 4(a). In the NS scenario this would mean that the core of the star would be much softer compared to the crust if described by the PNJL model rather than the NJL model.

The variation of the specific heat $C_V = T(\frac{\partial s}{\partial T})_V$, where $s = (\frac{\partial P}{\partial T})$ is the entropy density of the system, is shown in Fig. 4(b). For a crossover (here in the NJL model) the specific heat shows a peak. For a first order transition (here in the PNJL model) the C_V is discontinuous. Also we see that the specific heat in the PNJL model is lower than that in the NJL model for a general variation of μ_q and μ_e. A system described by the PNJL model is thus less susceptible to changing temperature than that described by the NJL model.

The variation of compressibility and specific heat shown here also captures the signature of a phase transition in the PNJL model and a crossover in the NJL model. Both

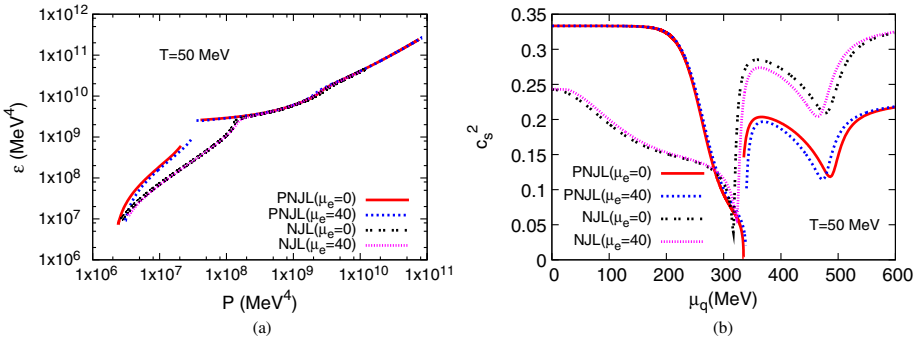

FIG. 3 (color online). (a) Equation of state and (b) isentropic speed of sound, for the NJL and PNJL models at $T = 50$ MeV.

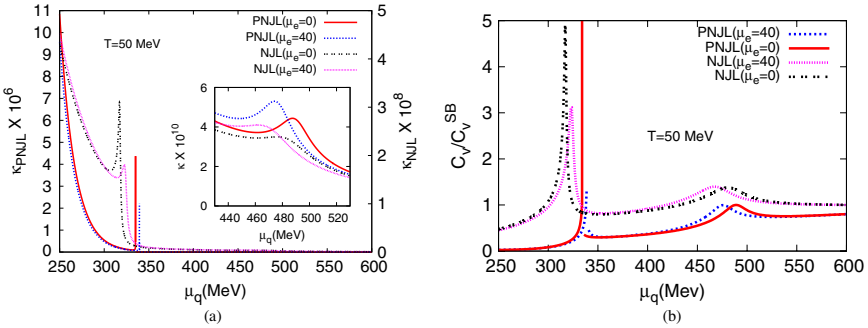

FIG. 4 (color online). (a) Variation of compressibility κ with μ_q. The peak around $\mu_q = 500$ MeV is shown in the inset where κ represents the compressibility in both the NJL and PNJL models. (b) Variation of specific heat scaled by its Stefan-Boltzmann value.

compressibility as well as specific heat are second derivatives of Ω and represent respectively the quark number fluctuations and energy fluctuations [37]. Discontinuity in compressibility as well as specific heat indicates a first order phase transition for the PNJL model. At $\mu_q \sim 500$ MeV, both the models exhibit a small peak due to the onset of melting of the strange quark condensate.

We now consider the net charge density given by $n_Q = \frac{2}{3}n_u - \frac{1}{3}n_d - \frac{1}{3}n_s - n_e$, where the number density of individual quarks and electrons is obtained from the relations $n_u = \frac{\partial\Omega}{\partial\mu_u}$, $n_d = \frac{\partial\Omega}{\partial\mu_d}$, $n_s = \frac{\partial\Omega}{\partial\mu_s}$, and $n_e = \frac{\partial\Omega_e}{\partial\mu_e}$. For $\mu_e = 0$, $n_e = 0$ and we have $n_u = n_d$. At large μ_q, the number density n_s of strange quarks becomes almost equal to the light quark number densities as the constituent masses of strange quarks are reduced significantly. So the net charge density n_Q will be close to zero and the system will become charge neutral asymptotically as shown in Fig. 5(a). At small μ_q, $n_Q \ll 1$ as the individual number densities themselves are exceedingly small. In fact this feature continues till the transition region where the light constituent quark masses drop sharply giving rise to nonzero number densities. Therefore n_Q shows a nonmonotonic behavior; rising from almost zero it reaches a maxima at certain μ_q determined mainly by the melting of the strange quark condensate and thereafter decreases steadily towards zero.

For higher μ_e, charge neutral configuration is possible even at nonzero moderate values of μ_q. For small μ_q, it is the n_e which dominates and keeps n_Q negative. As soon as n_u becomes large with increasing μ_q, n_Q goes through zero and becomes positive. Now since μ_s and μ_d are greater than μ_u due to β equilibrium, both n_s and n_d start to grow faster with the increase of μ_q. Finally at some μ_q the net charge becomes zero due to the mutual cancellation of n_u, n_d, and n_s, and thereafter it remains negative for higher μ_q as d and s quarks overwhelm the positively charged u quark. The electron number density is fixed for a fixed value of μ_e and T, and it is negligible compared to the quark number densities at high μ_q. The behavior of n_Q is similar for both the PNJL and NJL models though the actual values of the various chemical potentials for the charge neutrality conditions vary.

Given that one may be interested in the charge neutral condition, e.g., in the case of neutron stars, in Fig. 6 the charge neutral trajectories for the NJL model are compared with those of the PNJL model along with the phase diagrams. The trajectories are quite interesting in that they are closed ones pinned on to the μ_q axis. They start off close to $\mu_q = M_{\rm vac}$, the constituent quark mass in the model in vacuum. They make an excursion in the T-μ_q plane and join back at a higher μ_q. There is a maximum temperature T_Q up to which the trajectory goes. Beyond

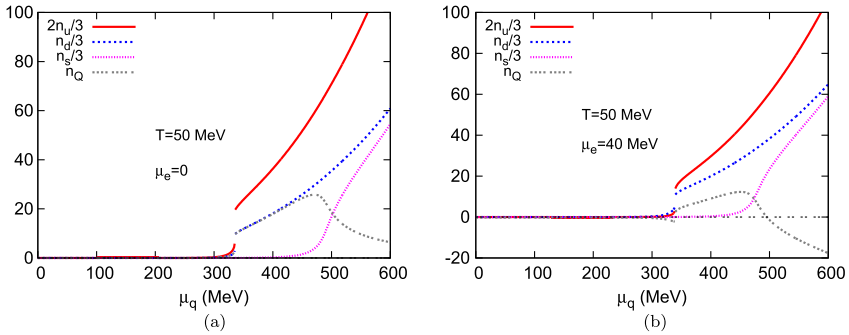

FIG. 5 (color online). Total charge and quark number densities scaled by T^3 as a function of quark chemical potential in the PNJL model.

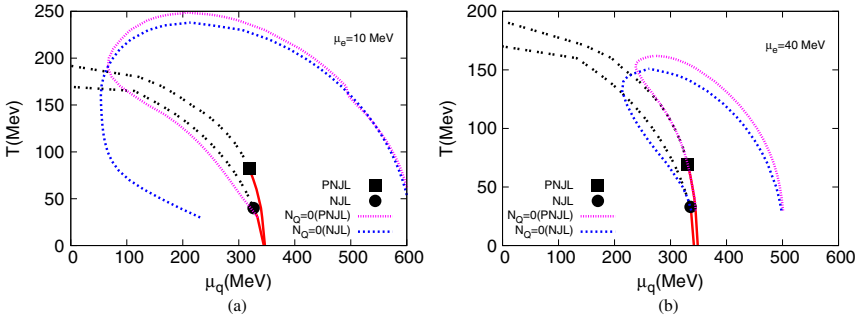

FIG. 6 (color online). Comparison of charge neutral trajectory in the NJL and PNJL models at (a) $\mu_e = 10$ and (b) $\mu_e = 40$.

this temperature no charge neutrality is possible. Below this temperature we have essentially two values of μ_q where charge neutrality occurs. There are significant differences between the contours of the NJL and PNJL models in the hadronic phase. However beyond the transition and inside the deconfined region, the differences subside as the Polyakov loop relaxes the confining effect leading to the PNJL model behaving in a similar way to that of the NJL model.

The behavior of the charge neutral contour is highly dependent on μ_e. With increasing μ_e the contour gradually closes in towards the transition line. For a given T there are two μ_q values where charge neutrality is obtained—one on the hadronic side and one on the partonic side. As a result of the closing in of the contour, these two values come closer to the transition line from opposite sides with increasing μ_e. The higher the μ_e, the closer we are to the transition region. Now suppose we are looking for an isothermal evolution of a system, or the isothermal configuration of a system such as the NS. Given the constraint of charge neutrality we would have a varying μ_e as the density profile changes. Similarly if μ_e is held constant then charge neutrality would not allow the temperature to remain fixed throughout and the evolution would take place along the contours described above. So in general a combination of T and μ_e is expected to maintain charge neutrality in a given system. A practical picture of NSs which have a profile of a low density crust that gradually increases in density to a highly condensed core would be that there is a complex profile for temperature and μ_e inside the NS. In fact if there exists a hadron-parton boundary, it may be either with high temperature or high electron density.

To contemplate this scenario in the light of the baryon densities achieved we plot the contours for constant baryon densities, scaled by the normal nuclear matter density ($n_0 = 0.15$ fm^{-3}) in Fig. 7 for $\mu_e = 40$ MeV. The charge neutral trajectories are also plotted along with the phase boundary. Obviously with increasing baryon (quark) chemical potential, baryon density would increase. What is interesting is the fact that high densities can also occur for lower chemical potential if the temperature is higher. For both the NJL and PNJL models at and above 3 times nuclear matter density the matter seems to be always in the partonic phase. A little below this density, matter may be in the partonic phase if it is at high temperature otherwise in the hadronic phase at low temperature. Thus the actual trajectory on the phase diagram would determine whether a hadron-parton boundary in the NS is in the mixed phase or in a state of crossover. Within the range of the charge neutral contour we find the baryon density increasing from a very small value to almost 10 times the normal nuclear matter density. If μ_e is increased further the baryon densities would also be much higher for a given μ_q. So if we assume local charge neutrality as well as an isothermal profile along a hadron-parton phase boundary, the baryon density close to the phase boundary may be too large. On the other hand for reasonable densities close to the phase

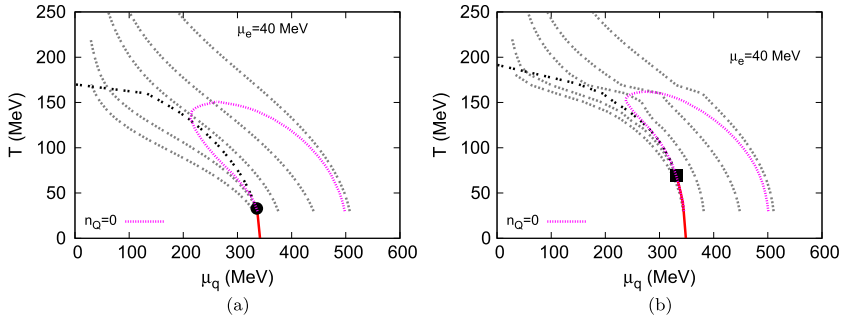

FIG. 7 (color online). The contour of scaled baryon number density n_B/n_0 (scaled by normal nuclear matter density) along with a phase diagram at $\mu_e = 40$ for (a) the NJL model and (b) the PNJL model (from left $n_B/n_0 = 0.5$, 1, 3, 5, 10, respectively).

boundary it would be impossible to maintain local charge neutrality along an isothermal curve. In that case it may be possible that the charge neutrality condition takes the system around the CEP to hold on to a reasonable density in the phase boundary region. This leads us to speculate that the transition in a NS itself may also be a crossover, quite unlike the picture in most of the studies of NSs.

The net strangeness fraction (n_s/n_B) along with n_B/n_0 is shown in Fig. 8. For a given temperature, there is a critical μ_q below which there is no net strangeness formation. At the critical μ_q a nonzero n_s/n_B occurs depending on the T. This strangeness fraction continues to appear at lower T for some higher μ_q. So a given strangeness fraction can occur only up to a certain critical temperature. The intersection of lines of constant baryon density and strangeness fraction indicates the possibility of evolution of a system to higher (lower) strangeness fraction with an increase (decrease) of T at a constant density. In the range of 5–10 times nuclear matter density we see that the strangeness fraction is increasing significantly towards unity indicating a possibility of formation of quark matter with an almost equal number of u, d, and s quarks. Similar results have also been found in other model studies [8]. Chunks of matter with $n_s/n_B = 1$, called strangelets, are expected to be stable (metastable up to weak decay) relative to nuclear matter in vacuum [40]. Investigation of these and various other properties of strange matter will be undertaken in future.

Usually the hydrodynamic evolution of a system is expected to follow a certain adiabat along which the entropy per baryon number (s/n_B) is a constant quantity. Among the various adiabats the system would choose one given its initial conditions. In the context of NSs, a fixed entropy per baryon is expected in a protoneutron star as well which is very different from a cold neutron star. It is usually hot and rich in leptons, i.e., electrons and trapped neutrinos. A few seconds after birth, the matter in the core of a hot NS has an almost constant lepton fraction (0.3–0.4) and entropy per baryon (1–2, in units of Boltzmann constant) [41,42]. The question as to whether the later evolution of the NS can be described to be one close to an adiabat is a matter of debate. On the other hand the commonly used approach of an isothermal evolution looks not quite favorable according to the above discussion on the charge neutrality condition.

The behavior of s/n_B in a plasma and in a hadron gas was analyzed within the framework of an extended bag model by Ref. [43]. A case study of such adiabats was done in the NJL model in Ref. [44]. It was found that unlike the prescription of adiabats meeting at the CEP given by Ref. [45], they meet close to the critical value of μ_q at $T = 0$ which is incidentally equal to the constituent quark mass M_{vac} in the model in vacuum. It was argued in Ref. [44] that as $T \to 0$, $s \to 0$ by the third law of thermodynamics. Hence in order to keep s/n_B constant, n_B should go to zero. This condition is satisfied when $\mu_q = M_{\text{vac}}$ of the theory. These authors also found similar results for the linear sigma model. In the PNJL model the introduction of a Polyakov loop produced a slight change in the configuration of the adiabats [46]. The constraint on the strangeness number to be zero also was found not to have a very significant effect [47].

The corresponding picture of isentropic trajectories with the condition of β equilibrium is shown in Fig. 9. Four cases are depicted here. Figures 9(a) and 9(b) show the cases with the $2 + 1$ PNJL model at $\mu_e = 0$ MeV and $\mu_e = 40$ MeV, respectively. From these two figures we find that the electron density does not have a significant effect on the isentropic trajectories. This means that the quark degrees of freedom seem to have a dominant effect in entropy over the electrons. The case with $n_s = 0$, i.e., effectively for a 2 flavor system, is shown in Fig. 9(c). In general the situation is similar. For small μ_q there is almost no change in Figs. 9(a) and 9(c) as both the cases are identical to 2 flavors. At intermediate values strange quarks start to pop out. Now the contours in Fig. 9(c) appear to be shifted and bent towards higher μ_q. This is because for 2 flavors a given baryon number density appears at a higher μ_q than that for $2 + 1$ flavors. Hence to get a fixed s/n_B the μ_q required is also higher. At even higher μ_q the thermal effects are negligible and hence s/n_B become almost

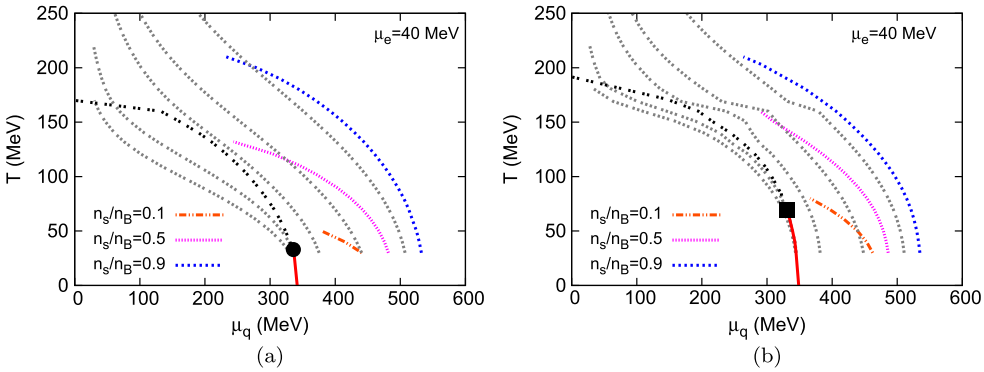

FIG. 8 (color online). The contour of the net strangeness fraction (n_s/n_B) along with n_B/n_0 at $\mu_e = 40$ for (a) the NJL model and (b) the PNJL model; the values of n_B/n_0 are 0.5, 1, 3, 5, and 10 (from left).

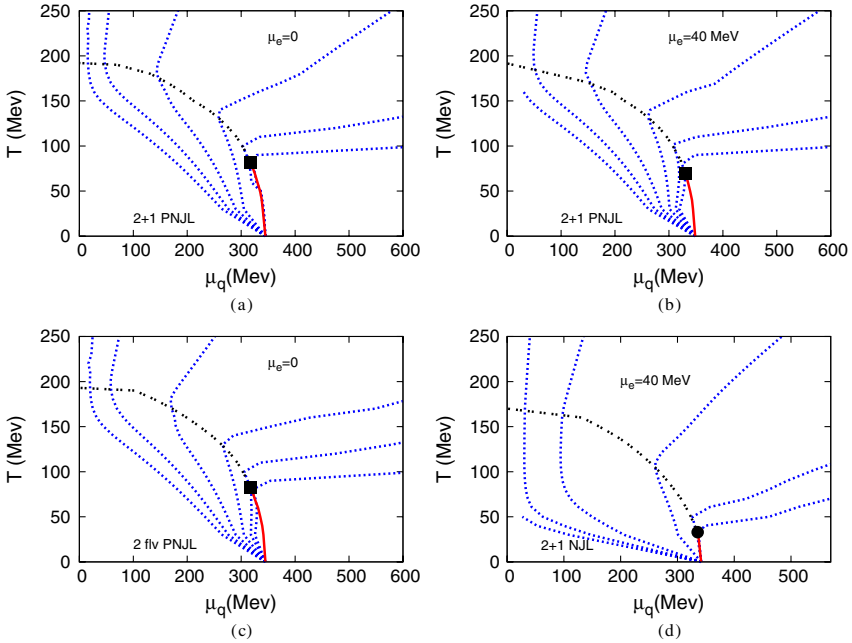

FIG. 9 (color online). The isentropic trajectories along with phase diagram for (a) at $\mu_e = 0$, 2 + 1 flavor PNJL, (b) at $\mu_e = 40$, 2 + 1 flavor PNJL, (c) at $\mu_e = 0$, 2 flavor PNJL, and (d) at $\mu_e = 40$, 2 + 1 flavor NJL model. $s/n_B = 300$, 100, 30, 10, 5, 3.5 (from left).

independent of the degrees of freedom. Thus again the contours become identical.

The results in the NJL model are significantly different from those of the PNJL model as can be seen by comparing the PNJL results with those of the NJL model shown in Fig. 9(d). Even for low T and μ_q there is a significant entropy generation as there is no Polyakov loop to subdue the same. Similar differences continue to appear even in the partonic phase.

Considering a system that has been compressed to a few times the nuclear matter density, it can try to relax back to lower densities along the adiabats. Interestingly the isentropic trajectories in the high density domain seem to behave as isothermals in the PNJL model. However as soon as the system converts into the hadronic phase, the adiabats drive it to a steep fall in temperature. We would like to mention that for a hadronic protoneutron star with beta equilibrated nuclear matter with nucleons and leptons in the stellar core, the EOS evaluated in Brueckner-Bethe-Goldstone theory was found to be similar for both isothermal and isentropic profiles [48].

In Ref. [49] isentropic trajectories were obtained in the PNJL model without the constraint of β equilibrium, for two different sets of parameters corresponding to an ultraviolet cutoff in the zero temperature integrals only (case I) and the same in all integrals (case II). Here we considered only the first case for regularization and find similar results.

While the possibility that a neutron star can be described using adiabatic conditions is a point to be pondered about, we note here that an excursion of the phase diagram of a β equilibrated matter is highly possible even in heavy-ion collisions to some extent. This is because both the isentropic lines as well as the characteristics of the phase boundary are quite similar for a wide variation of μ_e and μ_q. At the same time one should remember that in the laboratory conditions n_s is strictly zero. Anyway if a system is found to have traveled along an adiabat with $s/n_B \simeq 3$ to 4, it has most probably traversed close to the CEP. One can therefore try to correlate different observables like the enhancement of fluctuations of conserved charges and s/n_B to be in the above range to study the approach towards the CEP in heavy-ion collisions.

IV. SUMMARY AND CONCLUSION

In this paper we have studied the 2 + 1 flavor strongly interacting matter under the condition of β equilibrium. We have presented a comparative study of the NJL versus the PNJL model. The phase diagrams in these two models are broadly similar, but quantitatively somewhat different. The presence of the Polyakov loop delays the transition for larger values of temperature for a given quark chemical potential. As a result the CEP in the PNJL model is almost twice as hot as that in the NJL model. We have illustrated characteristics of the phase diagram with the behavior of some thermodynamic quantities like the constituent mass, compressibility, specific heat, speed of sound, and equation of state for $\mu_e = 0$ MeV and $\mu_e = 40$ MeV at $T = 50$ MeV. We found striking differences between the

NJL and PNJL model in terms of the softness of the equation of state in the hadronic and partonic phases.

The behaviors of electric charge and baryon densities in the two models also differ in the hadronic phases to some extent. The differences become less with increasing electron density. We explained how the charge neutral trajectory is important in deciding the path along which the core of the NS can change from hadronic to quark phase. For all values of μ_e we find that the contours are all closed ones and give a restricted range of temperature and densities that are allowed. We speculated a possible scenario in which the quark-hadron transition in a NS would be a crossover. Again the baryon density contours seemed to suggest that if a system has baryon density three times the nuclear matter density it is quite surely in the partonic phase. We also found that the strangeness fraction increases steadily with increasing baryon density, implying a possibility of having a strange NS.

The isentropic trajectories were obtained along which a system in hydrodynamic equilibrium is expected to evolve. The adiabats flow down from high temperature and low density towards low temperature and $\mu_q = M_{\text{vac}}$, the constituent quark mass in vacuum. The adiabats then steeply rise along the transition line, and thereafter go towards higher densities with almost a constant slope. For small s/n_B ratio the slope is so small that the isentropic trajectories almost become isothermal trajectories as well.

To summarize the scenario inside neutron stars we note that inside a newly born NS the temperature drops very quickly and gives rise to a system of low temperature nucleonic matter which may also be populated by hyperons and strange baryons due to high density near the core. The star is assumed to be β equilibrated and charge neutral. Now it is possible that due to some reason, e.g., sudden spin-down, this nucleonic matter will start getting converted to predominantly two flavor quark matter within a strong interaction time scale. This transition would start at the center and a conversion front moving outward will convert much of the central region of the star. Along the path of the conversion front, each point inside the star may lie on an isentropic trajectory. Gradually this system of predominantly 2 flavor quark matter will get converted to strange quark matter through weak interactions and finally a β equilibrated charge neutral strange quark matter will be produced. The strangeness production occurs mainly through nonleptonic decay [33]; the system is expected to lie on a constant density line and move towards the point with highest strangeness possible at that density. Finally the semileptonic processes will take over and the system will then evolve along a β equilibrated charge neutral contour.

The natural extension of the work is to obtain the detailed evolution of a family of neutron stars starting with different initial conditions and gravity effects incorporated. We hope to report the study in a future publication. It would also be important to consider colored exotic states like diquarks [50] that may arise at high densities.

ACKNOWLEDGMENTS

S. M. would like to thank CSIR for financial support. A. B. thanks UGC (DRS and UPE) and DST for support. R. R. thanks DST for support. We would like to thank Anirban Lahiri, Paramita Deb, and Sibaji Raha for useful discussion and comments.

[1] B. Müller, *The Physics of Quark Gluon Plasma*, Lecture Notes in Physics Vol. 225 (Springer, New York, 1985).
[2] K. Rajagopal and F. Wilczek, in *At the Frontier of Particle Physics: Handbook of QCD* (World Scientific, Singapore, 2001), Vol. 3, p. 2061.
[3] D. Blaschke, J. Berdermann, and R. Lastowiecki, Prog. Theor. Phys. Suppl. **186**, 81 (2010).
[4] N. K. Glendenning, J. Phys. G **23**, 2013 (1997).
[5] J. Schaffner-Bielich, Proc. Sci., CPOD07 (2007) 062 [arXiv:0709.1043].
[6] G. F. Burgio, M. Baldo, P. K. Sahu, A. B. Santra, and H.-J. Schulze, Phys. Lett. B **526**, 19 (2002); G. F. Burgio, M. Baldo, P. K. Sahu, and H.-J. Schulze, Phys. Rev. C **66**, 025802 (2002).
[7] M. Alford, M. Brady, M. Paris, and S. Reddy, Astrophys. J. **629**, 969 (2005).
[8] S. K. Ghosh and P. K. Sahu, Int. J. Mod. Phys. E **02**, 575 (1993).
[9] S. K. Ghosh, S. C. Phatak, and P. K. Sahu, Z. Phys. A **352**, 457 (1995).
[10] M. Buballa, Phys. Rep. **407**, 205 (2005).
[11] M. Baldo, M. Buballa, G. F. Burgio, F. Neumann, M. Oertel, and H.-J. Schulze, Phys. Lett. B **562**, 153 (2003) and references therein.
[12] K. Schertler, S. Leupold, and J. Schaffner-Bielich, Phys. Rev. C **60**, 025801 (1999).
[13] M. Baldo, G. F. Burgio, P. Castorina, S. Plumari, and D. Zappala, Phys. Rev. C **75**, 035804 (2007).
[14] C. Ratti, M. A. Thaler, and W. Weise, Phys. Rev. D **73**, 014019 (2006).
[15] S. K. Ghosh, T. K. Mukherjee, M. G. Mustafa, and R. Ray, Phys. Rev. D **73**, 114007 (2006).
[16] S. Mukherjee, M. G. Mustafa, and R. Ray, Phys. Rev. D **75**, 094015 (2007); S. K. Ghosh, T. K. Mukherjee, M. G. Mustafa, and R. Ray, *ibid.* **77**, 094024 (2008).
[17] A. Bhattacharyya, P. Deb, S. K. Ghosh, and R. Ray, Phys. Rev. D **82**, 014021 (2010).

[18] A. Bhattacharyya, P. Deb, A. Lahiri, and R. Ray, Phys. Rev. D **82**, 114028 (2010); **83**, 014011 (2011).
[19] S. B. Ruster, V. Werth, M. Buballa, I. A. Shovkovy, and D. H. Rischke, Phys. Rev. D **72**, 034004 (2005).
[20] M. Hanauske, L. M. Satarov, I. N. Mishustin, H. Stöcker, and W. Greiner, Phys. Rev. D **64**, 043005 (2001).
[21] P. Costa, M. C. Ruivo, Yu. L. Kalinovsky, and C. A. de Sousa, Phys. Rev. C **70**, 025204 (2004).
[22] P. Costa, M. C. Ruivo, and Yu. L. Kalinovsky, Phys. Lett. B **560**, 171 (2003).
[23] J. A. Pons, J. A. Miralles, M. Prakash, and J. M. Lattimer, Astrophys. J. **553**, 382 (2001).
[24] D. G. Yakovlev and C. J. Pethick, Annu. Rev. Astron. Astrophys. **42**, 169 (2004).
[25] D. G. Yakovlev, O. Y. Gnedin, M. E. Gusakov, A. D. Kaminker, K. P. Levenfish, and A. Y. Potekhin, Nucl. Phys. **A752**, 590 (2005).
[26] J. M. Lattimer and M. Prakash, Astrophys. J. **550**, 426 (2001).
[27] A. Bhattacharyya, I. N. Mishustin, and W. Greiner, J. Phys. G **37**, 025201 (2010).
[28] I. N. Mishustin, M. Hanauske, A. Bhattacharyya, L. M. Satarov, H. Stoecker, and W. Greiner, Phys. Lett. B **552**, 1 (2003).
[29] E. Witten, Phys. Rev. D **30**, 272 (1984).
[30] A. Bhattacharyya, S. K. Ghosh, P. Joarder, R. Mallick, and S. Raha, Phys. Rev. C **74**, 06580 (2006).
[31] C. Alcock, E. Farhi, and A. Olinto, Astrophys. J. **310**, 261 (1986).
[32] N. K. Glendenning, S. Pei, and F. Weber, Phys. Rev. Lett. **79**, 1603 (1997).
[33] S. K. Ghosh, S. C. Phatak, and P. K. Sahu, Nucl. Phys. **A596**, 670 (1996).
[34] L. McLerran, K. Redlich, and C. Sasaki, Nucl. Phys. **A824**, 86 (2009).
[35] K. Fukushima, Phys. Rev. D **77**, 114028 (2008).
[36] G. Y. Shao, M. Di Toro, B. Liu, M. Colonna, V. Greco, Y. X. Liu, and S. Plumari, Phys. Rev. D **83**, 094033 (2011); **84**, 034028 (2011).
[37] M. Iwasaki, Phys. Rev. D **70**, 114031 (2004).
[38] S. V. Molodtsov and Z. M. Zinovjev, Europhys. Lett. **93**, 11001 (2011).
[39] N. K. Glendenning, Phys. Rev. D **46**, 1274 (1992).
[40] E. Farhi and R. L. Jaffe, Phys. Rev. D **30**, 2379 (1984).
[41] A. Burrows and J. M. Lattimer, Astrophys. J. **307**, 178 (1986).
[42] D. Gondek, P. Haensel, and J. L. Zdunik, in *Protoneutron stars and constraints on maximum and minimum mass of neutron stars*, edited by K. L. Chan, K. S. Cheng, and H. P. Singh, ASP Conference Series Vol. 138, (Astronomical Society of the Pacific, Utah, USA, 1998), p. 131.
[43] A. Leonidov, K. Redlich, H. Satz, E. Suhonen, and G. Weber, Phys. Rev. D **50**, 4657 (1994).
[44] O. Scavenius, A. Mocsy, I. N. Mishustin, and D. H. Rishke, Phys. Rev. C **64**, 045202 (2001).
[45] M. Stephanov, K. Rajagopal, and E. Shuryak, Phys. Rev. Lett. **81**, 4816 (1998).
[46] T. Kahara and K. Tuominen, Phys. Rev. D **78**, 034015 (2008).
[47] K. Fukushima, Phys. Rev. D **79**, 074015 (2009).
[48] G. F. Burgio and H.-J. Schulze, Phys. At. Nucl. **72**, 1197 (2009).
[49] P. Costa, H. Hansen, M. C. Ruivo, and C. A. de Sousa, Phys. Rev. D **81**, 016007 (2010).
[50] N. Bentz, T. Horikawa, N. Ishii, and A. W. Thomas, Nucl. Phys. **A720**, 95 (2003); S. Roessner, C. Ratti, and W. Weise, Phys. Rev. D **75**, 034007 (2007).